Accepted Manuscript

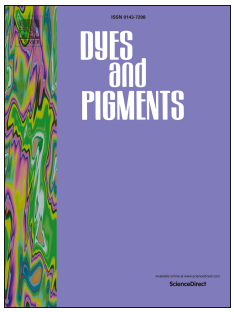

Chlorin derivatives sterically-prevented from self-aggregation with high antitumor activity for photodynamic therapy

Irwin A.P. Linares, Kleber T. de Oliveira, Janice Rodrigues Perussi

PII: S0143-7208(17)30665-4

DOI: 10.1016/j.dyepig.2017.06.011

Reference: DYPI 6032

To appear in: *Dyes and Pigments*

Received Date: 30 March 2017

Revised Date: 25 May 2017

Accepted Date: 7 June 2017

Please cite this article as: Linares IAP, de Oliveira KT, Perussi JR, Chlorin derivatives sterically-prevented from self-aggregation with high antitumor activity for photodynamic therapy, *Dyes and Pigments* (2017), doi: 10.1016/j.dyepig.2017.06.011.

Chlorin derivatives sterically-prevented from self-aggregation with high antitumor activity for photodynamic therapy

Irwin A. P. Linares[a],Kleber T. de Oliveira[b] and Janice Rodrigues Perussi[a]

[a]Instituto de Química de São Carlos, Universidade de São Paulo, São Carlos-SP, Brazil

[b] Departamento de Química, Universidade Federal de São Carlos, São Carlos-SP, Brazil

Corresponding author address:

Instituto de Química de São Carlos, Universidade de São Paulo**,** Av. Trabalhador São-Carlense, 400. São Carlos-SP, Brazil.

13560-970

*janice@usp.br

Abstract

In this study two new chlorin derivatives sterically prevented from aggregation were synthesised by the Diels-Alder reaction originated from protoporphyrin IX dimethyl ester and 1-(2-hydroxyethyl)maleimide. The compounds were fully characterised by ^{1}H-NMR, ^{13}C-NMR, UV-Vis and high-resolution mass spectroscopy (HRMS) and their photochemical properties such as singlet oxygen quantum yield (ϕ_0), fluorescence quantum yield (ϕ_f) and photodegradation were also evaluated. Furthermore, the partition coefficient (log P) revealed that these compounds present amphiphilic properties. Studies

of the photodynamic action in tumour cells (HEp-2 and HeLa) and non-tumour cells (Vero) were also performed in order to confirm the photodynamic therapy (PDT) activity that was indicated by the preliminary photophysical studies. Those phototoxicity results were 55–77% higher than the results obtained with the commercial photosensitiser verteporfin. Finally, cytotoxic assays were performed with the new photosensitiser candidates and cell death was determined using fluorescence microscopy, which provided information about the mechanisms of cell death. In general, we have obtained improved and accessible compounds for PDT studies, as highlighted by the research presented here.

Keywords: Chlorins, aggregation, amphiphilic character, photobleaching, phototoxicity, mechanism of cell death

Highlights

New chlorin derivatives, sterically prevented from aggregation, were synthesised by the Diels-Alder reaction.

Chlorin derivatives exhibit no aggregation in an aqueous medium (phosphate-buffered saline).

The cytotoxicity of the chlorin derivatives in the tumour cells is higher than verteporfin.

The mechanism of cell death occurs via an apoptotic process in three cell lines after irradiation.

1. Introduction

Photodynamic therapy (PDT) is a non-invasive therapeutic method that induces cell death of tumour cells by apoptosis or necrosis. The therapy uses dyes or pigments (photosensitiser) that are capable of absorbing visible light energy and transferring part of the absorbed energy to adjacent molecules. The transfer of energy is usually to the oxygen (O_2) molecules which are present in the tissues. This process leads to a series of photochemical reactions that produce singlet oxygen, which is extremely toxic, and other reactive oxygen species and free radicals, thus resulting in a strong cytotoxic effect and tumour cell death [1–5].

Different types of photosensitisers, for example, porphyrin [6–8], chlorin [9–11] and phthalocyanine [12, 13] derivatives, have been used in PDT studies. Hematoporphyrin derivative (HpD) and Photofrin® are considered to be part of the first generation of photosensitizers used in the therapy against cancer. However, the strong aggregation of these photosensitizers in physiologic medium, the low singlet oxygen quantum yields, and the short penetration of red light (typically 630 nm) has resulted in limited use of these light-absorbing molecules. Those limitations have led to the development of a new generation of compounds with improved physical, chemical and photobiological properties [14].The most recent generation of compounds was developed to exhibit characteristics such as intense absorption bands at longer wavelengths and shorter skin photosensitivity periods, which would enable the treatments to reach deeper tissues compared to the first generation of photosensitisers [15].

Chlorin derivatives, when compared with porphyrins, have a reduced double bond in one β-position of one tetrapyrrolic ring [16, 17], resulting in a red-shifted absorption band (640 to 680 nm) and allowing deeper light penetration in the tissue [18–20]. Several chlorins have been approved for clinical use: Foscan®, talaporfin (NPe6) and verteporfin (Visudyne®) [21, 22]. Visudyne® is derived from the natural protoporphyrin IX (PpIX) (Figure 1) [23–25]. It is used in the treatment of age-related macular degeneration, choroidal neovascularization due to secondary pathological myopia, and suspected ocular histoplasmosis [26, 27]. In the last 15 years, this photosensitizer has been used as an efficient compound in PDT studies and in clinical treatments for macular degeneration [28].

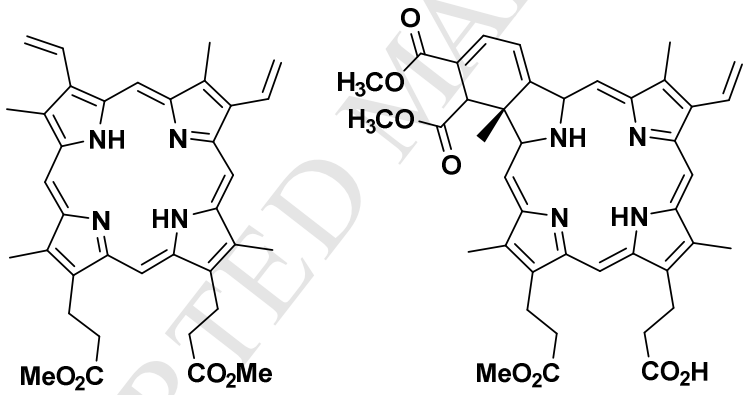

Protoporphyrin IX dimethyl ester **Visudyne**

Fig. 1. Protoporphyrin IX analogues.

Several approved photosensitisers, for example, Photofrin® [29, 30], Foscan [31, 32], Laserphyrin [33, 34] and SnET2 [35, 36], are limited in their ability to be applied to PDT because of skin photosensitivity caused by the slow clearance of photosensitisers from the organism, low solubility, penetration of light and low tumour-targeting efficacy [37]. Therefore, there are great challenges for

synthetic organic chemistry researchers to improve photosensitisers for PDT treatments.

Different approaches have been used for the synthesis of chlorins derived from PpIX dimethyl ester, which has resulted in better solubility and non-aggregation in physiological medium [38–41]. Recently, chlorin derivatives synthesised by the Diels-Alder reaction between diene-appended porphyrins and maleimides yielded L-shape chlorin derivatives. These L-shape structures prevent the aggregation caused by the strong attraction between the π-systems of the polyaromatic heterocycles, thus resulting in molecules with high singlet oxygen quantum yields [39, 41]. Therefore, in this study, we carried out the synthesis of a new chlorin derivatives by the Diels-Alder reaction between the PpIX dimethyl ester and different maleimides. We characterised the new photosensitiser derivatives and investigated their photodynamic activity, cytotoxicity, phototoxicity, photobleaching, cell death and accumulation in cells.

2. Materials and Methods

2.1 Reagents and measurements

All reagents were of analytical grade and were purchased from Aldrich or national suppliers. Solvents and reagents that were used for the synthesis were only used after purification according to standard procedures [42]. Ultrasound irradiation was used to deoxygenate the toluene for the Diels-Alder reactions. ^{1}H and ^{13}C-NMR spectra were recorded on a Bruker Avance 400 spectrometer at 400.13 MHz and 100.13 MHz, respectively, using $CDCl_3$ as the solvent and

tetramethylsilane (TMS) as the internal reference. The chemical shifts were expressed in parts per million (ppm) and the coupling constants (J) in hertz (Hz). High-resolution mass spectrometry (HRMS) analyses were obtained using the ESI-LTQ orbitrap (Thermo Scientific) and Xcalibur 2.1 analysis processing software. The UV-Vis absorption spectra analyses of the chlorin derivatives were performed using a Perkin Elmer Lambda 25 spectrophotometer.

Preparative purifications were carried out by using column chromatography and silica gel 200 and 400 mesh, and preparative thin-layer chromatography (TLC) and analytical TLC were conducted on TLC Silica gel 60 aluminium sheets (1mm thick) (Merck). The light-source for photobleaching was a 660 nm diode laser (FTC 500, OPTO, Sao Carlos-SP, Brazil) in the PDT/iPDT mode.

The partition coefficients and fluorescence measurements of the chlorin derivatives were performed using a spectrophotometer (HITACHI U-2800, Japan) and a spectrofluorometer (HITACHI F-4500, Japan), respectively, with 10 mm path length quartz cuvettes. The light-source used for the photodynamic treatment was an irradiation table called Biotable that contained a series of 660 ± 10 nm LEDs with a fluence rate of 27.6 $mWcm^{-2}$ (LAT, IFSC-USP). The absorbance measurements of the formazan dye after the phototoxic assays were read in a Biotek-Synergy HT spectrophotometer. To visualise cell death, a fluorescence microscope (Olympus BX41) was used with the following parameters: 20X magnification, excitation filter of 460/90 nm, dichromatic mirror of 50 nm and barrier filter of 520 nm. Images were captured with an Olympus DP72 digital camera.

2.2 Synthesis of 4,10-Dioxatricyclo[5.2.1.0]dec-8-ene-3,5-dione (**3**)

The synthesis of 4,10-Dioxatricyclo[5.2.1.0]dec-8-ene-3,5-dione (**3**) was carried out following methods reported in a previous publication [43]. In a 100 mL round-bottom flask, maleic anhydride (**1**) (10.00 g, 102 mmol), toluene (50 mL), and furan (**2**) (7.5 mL, 103.1 mmol) were stirred at room temperature under an inert atmosphere for 24 h. The product was obtained after filtration and washing of the precipitate with cold diethyl ether (80% yield, 13.57 g, 81.73 mmol). ^{1}**H-NMR** (400 MHz, DMSO-d_6) δ 6.56 (s, 2H), 5.32 (s, 2H), 3.29 (s, 2H); ^{13}**C-NMR** (100 MHz, DMSO-d_6) δ 172.0, 137.3, 82.1, 49.5.

2.3 Synthesis of 4-(2-Hydroxy-ethyl)-10-oxa-4-aza-tricyclo [5.2.1.0]-dec-8-ene-3,5-dione (**4**)

The synthesis of 4-(2-Hydroxy-ethyl)-10-oxa-4-aza-tricyclo [5.2.1.0]-dec-8-ene-3,5-dione (**4**) was carried out following methods reported in a previous publication [44]. A 50 mL two-neck round-bottom flask was adapted with a reflux condenser, the intermediate **3** (5.0 g, 30.1 mmol) was combined with dry methanol (15 mL). After stabilizing the magnetic stirring and the reaction temperature at 0°C, ethanolamine was added dropwise (1.84 g, 30.12mmol). The mixture was refluxed for 24 h. The methanol was then distilled off under reduced pressure, and the product was recrystallised from diethyl ether at -20°C. The crystals were collected by filtration and washed with cold diethyl ether in 61% yield. (3.81 g, 18.21 mmol). ^{1}**H-NMR** (400 MHz, DMSO-d_6) δ 6.53

(s, 2H), 5.10 (s, 2H), 3.39 (s, 4H), 2.90 (s, 2H); ^{13}**C-NMR** (100 MHz, DMSO-d_6) δ 176.9, 136.9, 80.7, 57.7, 47.6, 41.0.

2.4 Synthesis of 1-(2-Hydroxyethyl)-1H-pyrrole-2,5-dione (**5**)

The synthesis of 1-(2-Hydroxyethyl)-1H-pyrrole-2,5-dione (**5**)was carried out following methods reported in a previous publication [43]. In a50 mL round-bottom flask adapted with a flux condenser and magnetic stirring, the intermediate **4** (2.30 g, 10.99 mmol) was combined with toluene (30 mL). The reaction was refluxed for 7 h. The resulting mixture was immediately filtered, and the product crystallised from toluene in 81% yield(1.25 g, 8.87 mmol). ^{1}**H-NMR**(400 MHz, DMSO-d_6) δ7.01(s, 2H), 4.78 (br, 1H), 3.46 (br, 4H); ^{13}**C-NMR** (100 MHz, DMSO-d_6) δ171.1, 134.5, 57.9, 39.9.

2.5 Synthesis of protoporphyrin IX dimethyl ester (**7**)

The synthesis of protoporphyrin IX dimethyl ester (**7**) was carried out following methods reported in a previous publication [39]in75% (1.59 g, 2.70 mmol).^{1}**H-NMR** ($CDCl_3$, 400 MHz) δppm: -3.69 (s, 2H), 3.28 (t, 4H, J = 7.7 Hz); 3.56 (s, 3H); 3.61 (s, 3H); 3.62 (s, 6H), 3.65 (s, 3H); 3.70 (s, 3H); 4.34 (t, 4H, J =7.7 Hz); 6.16 (d, 2H, J =11.5 Hz); 6.35 (d, 2H, J =17.8 Hz), 8.27 (dd, 2H, J =17.9 Hz, J =11.3 Hz); 9.92 (s, 3H); 9.93 (s, 1H); 10.05 (s, 3H); 10.06 (s, 3H).

2.6 Diels-Alder reaction between protoporphyrin IX dimethyl ester (**7**) and 1-(2-Hydroxyethyl)-1H-pyrrole-2,5-dione (**5**)

The syntheses were carried out following the modification of a procedure that has been previously published [39]. In a glass pressure tube, were added **7** (60 mg, 0.1 mmol), dry toluene (5 mL) and **5** (282 mg, 2 mmol). The reaction was stirred at 125^{o}C for 24 h. The reaction was monitored by TLC and UV-Vis spectroscopy in order to verify the consumption of the starting material. The reaction products were purified by flash column in silica gel, and preparative TLC chromatography using chloroform, ethyl acetate and methanol in a 5:4:1 ratio as eluent. Two chlorin derivatives, **8-a** and **8-b**, were crystallised from CH_2Cl_2 and hexane in 33 and 34%, respectively.

2^1,2^2[N,N-dicarbonil-N-4-(2-hydroxyethyl)phenyl]-13,17-bis[2-(methoxycarbonyl)ethyl]-2,7,12,18-tetramethyl-8-vinyl-2,2^1,2^2,2^3-tetrahydrobenzo[b]porphyrin (**8a**): **^{1}H-NMR** ($CDCl_3$, 400 MHz) δ (ppm): -2.49 (s, 2H,); 2.01 (s, 3H); 3.13 - 3.17 and 3.20 - 3.24 (m, 9H); 3.40 (s, 3H); 3.42 - 3.45 (m, 2H); 3.50 (s, 3H); 3.54 (s, 3H); 3.66 and 3.69 (s, 6H); 3.75 - 3.79 (m, 1H); 4.18 (t, 2H, J=7.8 Hz); 4.31 (t, 2H, J=7.7 Hz), 4.51 (d, 1H, J=8.4 Hz); 6.15 (dd, 1H, J=1.4 Hz, J=11.5 Hz); 6.34 (dd, H, J=1.4 Hz and J=17.8 Hz); 7.35 (t, 1H, J=5.3 Hz); 8.17 (dd, 1H, J=17.8 Hz and 11.5 Hz); 9.07 (s, 1H); 9.30 (s, 1H); 9.70 (s, 1H), 9.86 (s, 1H); **^{13}C-NMR** ($CDCl_3$, 100 MHz) δ (ppm): 11.4, 11.6; 12.3, 21.5,21.9, 25.6, 26.5,36.6, 37.0, 38.5, 50.1, 51.7, 51.8, 52.3, 90.4, 93.4, 97.9, 99.8, 115.6, 121.4, 129.2, 129.8, 130.9, 132.6, 133.7, 133.9, 136.2, 136.5, 138.3, 139.6, 149.5, 151.0, 151.3, 152.2, 165.9, 173,4, 173.8,174.8,178.5;

HRMS (ESI-LTQ orbitrap velos): m/z calculated for $[M+H]^+$ 732.33716, found 732.33918.

2^1,2^2[N,N-dicarbonil-N-4-(2-hydroxyethyl)phenyl]-8,12-bis[2-(methoxycarbonyl)ethyl]-2,7,12,18-tetramethyl-8-vinyl-2,2^1,2^2,2^3-tetrahydrobenzo[b]porphyrin (**8b**): **^{1}H-NMR** ($CDCl_3$, 400 MHz) δ (ppm): -2.45 (s, 2H,); 2.01 (s, 3H); 3.13 - 3.18 and 3.20 - 3.25 (m, 9H); 3.41 (s, 3H); 3.41 (s, 3H);3.45 (s, 3H); 3.50 - 3.57 (m, 2H); 3.62 (s, 3H); 3.64 and 3.65 (s, 6H); 3.74 e 3.79 (m, 1H); 4.17 (t, 2H, J=7.8 Hz); 4.30 (t, 2H, J=7.7 Hz), 4.50 (d, 1H, J=8.4 Hz); 6.12 (dd, 1H, J=1.4 Hz, J=11.5 Hz); 6.34 (dd, H, J=1.4 Hz, J=17.8 Hz); 7.34 (t, 1H, J=5.4 Hz); 8.13 (dd, 1H, J=6.3 Hz and 17.8 Hz); 9.23 (s, 1H); 9.24 (s, 2H), 9.69 (s, 1H), 9.76 (s, 1H); **^{13}C-NMR** ($CDCl_3$, 100 MHz) δ (ppm): 11.2, 11.7, 12.4, 21.6, 21.9, 25.6, 26.6, 36.7, 37.1, 38.6, 50.1, 51.7, 51.8, 52.2, 89.9, 94.1, 98.4, 99.4, 116.0, 120.9, 129.9, 130,4, 131.2, 133.3, 133.8, 135.9, 136.8, 137.3, 138.0, 139.7, 149.6, 150.6, 151.4, 152.8, 165.6, 173.4, 173.8, 174.7, 178.5; **HRMS (ESI-LTQ orbitrap velos)**: m/z calculated for $[M+H]^+$ 732.33698, found 732.33918.

2.7 Singlet oxygen quantum-yield measurement

The singlet oxygen quantum yields (Φ_Δ) of **8-a** and **8-b** were determined from the intensity of the phosphorescence decay at 1270 nm [45]. The data were recorded with a time-resolved NIR fluorometer (Edinburgh Analytical Instruments) at the Departamento de Bioquímica, Instituto de Química, Universidade de São Paulo. The NIR fluorimeter was equipped with an Nd:YAG

LASER (Quantel) and a system optical parameter oscillator (OPO) allowing to choose the desired wavelength in which the samples were excited at 420 nm (5 ns pulse). The emitted light was passed through silicon, an interference filter and a monochromator before detection with an NIR photomultiplier (Hammamatsu Co. R5509). The singlet oxygen lifetime was determined by applying first-order exponential fittings to the phosphorescence decay curve. The Φ_Δ values were obtained using verteporfin as a reference (Φ_Δ=0.77) [46]. This procedure was performed in triplicate.

2.8 Fluorescence quantum yield measurements

The fluorescence quantum yields were determined using Rhodamine B in ethanol as a reference (Φ_f = 0.65) [47]. The solutions of the chlorin derivatives, **8a** and **8-b,** were prepared in DMSO from stock solutions. The absorbance was maintained at approximately 0.04 and 0.05 to avoid the inner filter effect. Excitation of both chlorins was performed at 510 nm, and the emission spectra were recorded. This procedure was performed in triplicate.

2.9 Photobleaching studies

A solution of **8-a** or **8-b** was prepared in CH_2Cl_2 with an absorbance value of approximately 1. The solution was irradiated at 661 nm for 10 minutes, with 1 min intervals, using a laser potency of 50 mW. The absorbance spectra were monitored after each irradiation interval in order to observe whether photobleaching of the chlorin derivatives occurred [17].

2.10 Determination of the partition coefficients in a solution of 1-octanol and PBS

The partition coefficients were determined at room temperature by a spread shake-flask method [48].The phosphate-buffered saline (PBS) and 1-octanol were mixed for five days to promote solvent saturation in both phases. Compounds **8-a** or **8-b** were dissolved in the organic phase. Subsequently, equal amounts of PBS, 1-octanol and photosensitisers at 1.0×10^{5} mol L^{-1} were mixed for 3 h under magnetic stirring and protection from light. The phase separation was followed by 10 min of centrifugation at 1000 rpm. The UV-Vis absorption spectra were measured before and after partitioning, and the differences were measured at the Soret band.

2.11 Aggregation study

Tetrapyrrolic molecules, such as chlorin derivatives, frequently aggregate in an aqueous medium due to the strong attractive interactions between the π-systems of the polyaromatic compound and the low interaction with the solvent. To evaluate the aggregation process, compounds **8-a** or **8-b** and verteporfin, were evaluated in different concentrations. Each sample solution was prepared in DMSO and PBS in order to determine the presence or absence of aggregation in solution. UV-Vis analyses were monitored for changes in the λ_{max} band of the spectra.

2.12 Phototoxicity assay

In this study, two cell lines were used: HeLa cell line (CCL-2^{TM}, ATCC, USA), a human cervical carcinoma cell, and HEp-2 (CCL-23^{TM}), an epithelial tumour-cell line. These cell lines were grown in Iscove's Modified Dulbecco's media (Sigma-Aldrich) and were supplemented with 10% foetal bovine serum (FBS, Cultilab) and 0.01% antibiotics (penicillin and streptomycin, Cultilab) in 75 cm^2 cell culture flasks incubated at 37°C and 5% CO_2. The cells were seeded ($5x10^4$ cells mL^{-1}) in 96-well plates and underwent photodynamic treatments. Cell viability was evaluated using the MTT (3,4,5-dimethylthiazol-2,5-diphenyl tetrazolium bromide) assay [49]. This method is based on the ability of viable cells with active metabolisms to use mitochondrial dehydrogenase enzymes to cleave the tetrazolium rings of the yellow MTT and form an insoluble precipitate (formazan crystals) inside of the cells [50]. Cells were incubated for 2 h in the absence of light with the photosensitisers and different concentrations of **8-a** and **8-b**. Subsequently, the cells were irradiated at 660 ± 10 nm using the Biotable at two time intervals in order to obtain two different light doses: 3.0 and 6.0 J cm^{-2}.

At 48 h post-irradiation, the medium was removed and the cells were incubated for 3 h with an MTT solution in culture medium added to each well of the plate. Following the incubation period, the solution that contained MTT was removed and the cells washed with 100 µL PBS. The formazan crystals were solubilised in 100 µL of absolute ethanol and 100 µL of isopropyl alcohol. The absorbance was read at 570 nm. The cell survival rate (%) was assessed in relation to the photosensitiser concentration. The average inhibitory

concentrations (IC_{50}) of the photosensitisers were determined. We also carried out an analysis of controls with no treatment, cells treated only with photosensitisers (not irradiated), and cells treated only with irradiation (without photosensitiser).

2.13 Cell death detection by acridine orange/ethidium bromide (AO/EB) staining

HeLa and Hep-2 cells were seeded ($5x10^4$ cells mL^{-1}) in sterile chamber slides with culture medium. After 24 h the cells were incubated with different concentration of **8-a** or **8-b** for 2 h. After the incubation period, the cells were washed with PBS, maintained in culture medium, and then irradiated with a light dose of 3 or 6 J cm^{-2}. After 48 h, the cells were stained with a mixture of ethidium bromide and acridine orange (100 µg mL^{-1}). The labelled cells were visualised by fluorescence microscopy [51].

2.14 Statistical Analysis

The data from the biological assays were analysed by one-way analysis of variance (ANOVA) followed by Student-Newman-Keuls multiple-comparisons test (Graph Pad InStat software). Differences were considered significant when $p \leq 0.05$.

3. Results and discussion

3.1 Chlorin derivatives syntheses

The preparation of protoporphyrin IX dimethyl ester (PpIX) (**7**), described in scheme 1, began with a process of elimination of two hydroxyl (-OH) groups of hematoporphyrin (Hp) (**6**). Then, an esterification in the presence of methanol and sulfuric acid (H_2SO_4) (5%) was performed maintaining the protection from light. The final product **7** was obtained after solvent evaporation and a simple crystallization from $CHCl_3$:MeOH (1:3). Compound **7** was isolated in 79% yield and characterised by ^{1}H-NMR and UV-Vis in order to confirm its identity and purity.

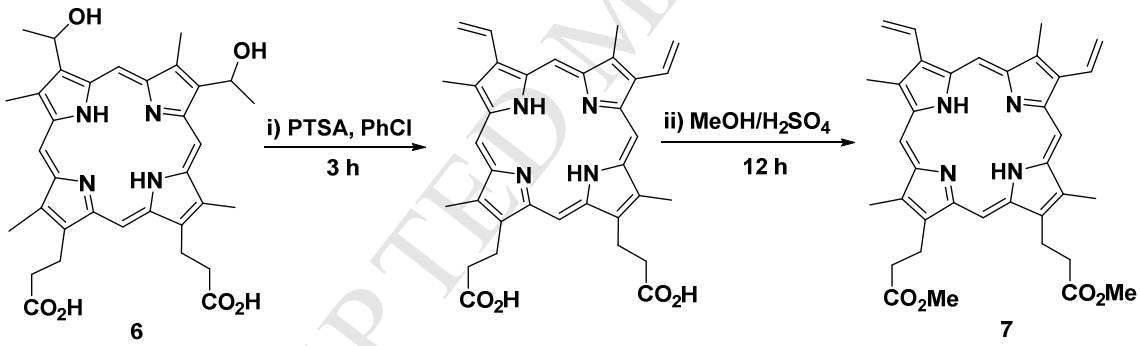

Scheme 1. Synthesis of protoporphyrin IX dimethyl ester from hematoporphyrin.

After obtaining **7**, the synthesis of the dienophile maleimide **5** was performed, as described in scheme 2. For this purpose, the Diels-Alder adduct, **3**, was obtained from maleic anhydride (**1**) and furan (**2**) (80% yield) [43]. Next, ethanolamine was added to compound **3**, yielding the maleimide **4** (61%) [44]. Compound **5** was obtained after a retro-Diels-Alder reaction in 81%yield [43]. The Diels-Alder reaction between **5** and **7** was performed in glass-pressure

tubes (toluene at 125°C, 24h), and catalytic amounts of BHT were used to avoid polymerised by-products (Scheme 3).

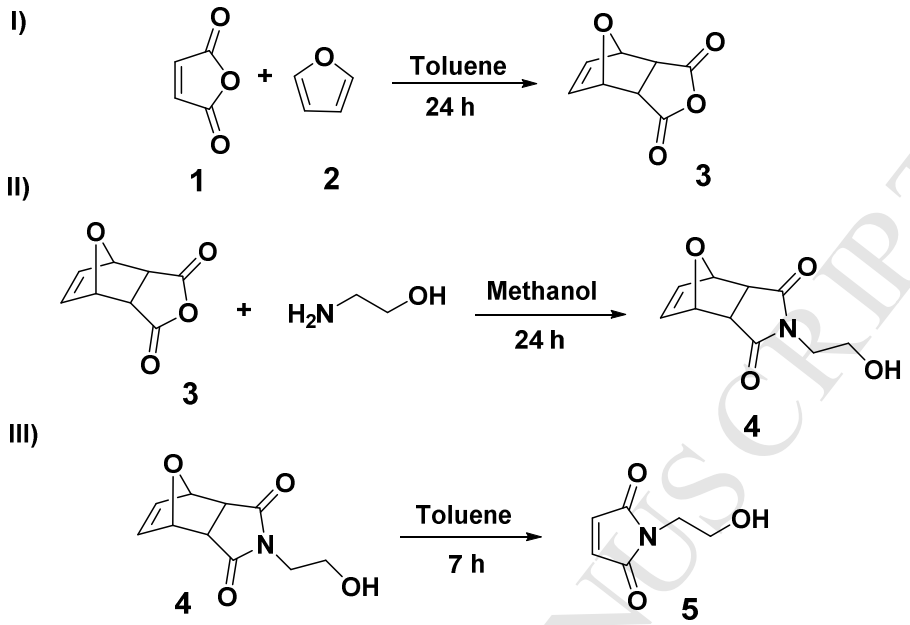

Scheme 2. Synthesis of N-(hydroxyethyl)maleimide.

The chlorin derivatives **8-a** and **8-b** were separated by preparative TLC over silica at a 1:1 ratio, resulting in 68% overall yield. These compounds were fully characterised by ^{1}H-NMR, ^{13}C-NMR, HRMS and UV-Vis.

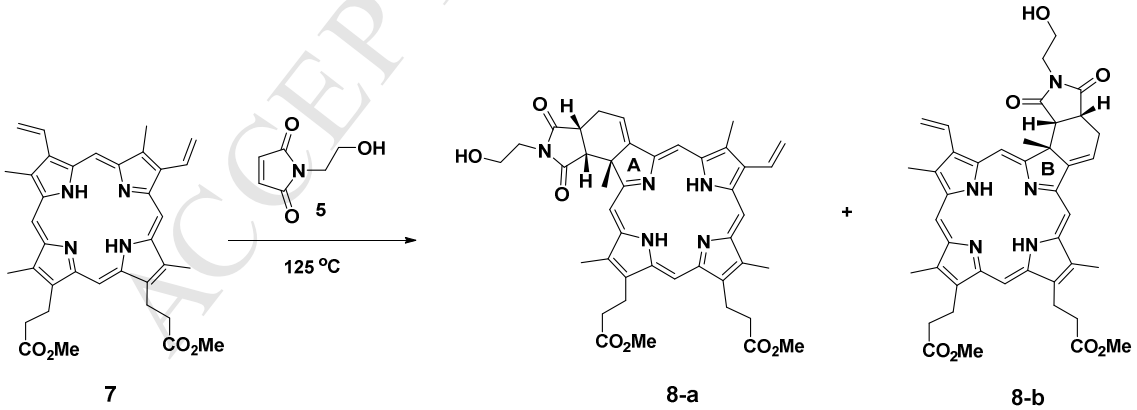

Scheme 3. Synthesis of chlorins **8-a** and **8-b**.

3.2 Singlet Oxygen Quantum Yields (Φ_Δ) measurements

The singlet oxygen quantum yields of **8-a**, **8-b** and verteporfin (standard) were determined from equation (1). This term is used to describe the measurement of the efficiency in which molecules are able to absorb light and convert molecular oxygen ($^3O_2$) to singlet oxygen ($^1O_2$) [52].

$$\Phi_\Delta = \frac{Abs_{Std}}{Abs_{PS}} \frac{I_{PS}}{I_{Std}} \frac{\tau_{Std}}{\tau_{PS}} \Phi_\Delta^{Std} \quad (1)$$

Where (Φ_Δ) represents the singlet oxygen quantum yield of the sample and (Φ_Δ^{Std}) is the standard (Verteporfin) singlet oxygen quantum yield. Abs^{PS} and Abs^{Std} are the absorbance values of the photosensitiser samples and the standard. I_{abs} and I_{abs}^{Std} are the maxima intensity of phosphorescence decay curve for the sample and the standard. τ_{PS} and τ_{Std} are the single-oxygen lifetime of the sample and the standard, respectively. The solutions of **8-a**, **8-b** and verteporfin were solubilised in DMSO. The chlorins **8-a** and **8-b** showed similar singlet oxygen quantum yields when compared to verteporfin (Table 1).

Table 1. Quantum yield values of singlet oxygen formation (Φ_Δ) and fluorescence (Φ_f) of verteporfin and of chlorins **8-a** and **8-b**. Data are expressed as average ± SD.

	(Φ_Δ)	**(Φ_f)**
Verteporfin	0.77 ± 0.02[46]	0.0085 ± 0.0006 $^{\alpha}$
8-a	0.75 ± 0.02	0.0096 ± 0.0003
8-b	0.73 ± 0.03	0.0110 ± 0.0006*, $^{\alpha}$

Experiment was performed in triplicate at 20°C
$^{\alpha}$ Statistically significant difference from CHL-OH-A ($p<0.05$)
* Statistically significant difference from Verteporfin ($p<0.01$)

3.3 Fluorescence Quantum yields (Φ_f) measurements

The fluorescence quantum yield is defined as the number of emitted photons relative to the number of absorbed photons and was determined using equation (2) [53].

$$\Phi_f = \Phi_f^{Std} \frac{F \,.A_{Std} \,.n^2}{F_{Std} \,.A \,.n_{Std}^2} \quad (2)$$

Where (Φ_f^{Std}) represent the fluorescence quantum yield of the standard. F and F_{Std} represent the areas under the fluorescence emission curves for the sample and standard, respectively. A and A_{Std} are the absorbance of the chlorin derivatives and the standard acquired from the same amount of solution used to measure the fluorescence emission spectra of both. The parameter, n and n_{Std} are the refractive indices for the used solvents. Solutions of each compound, **8-a**, **8-b**, were prepared in DMSO and exhibited emissions at 676 nm with quantum yield of fluorescence values comparable to the verteporfin (standard) (table 1).

3.4 Photobleaching studies

Photostability is a physicochemical property important to photosensitisers in general, since during the irradiation time, the molecule may lose its photodynamic activity due to chemical changes in its structure resulting in small fragments (photo-products) that have no appreciable absorption in the visible region [54]. The synthesised compounds **8-a** and **8-b** showed a slight

photobleaching effect, depending on the irradiation time. A reduction of approximately 5% in the absorbance band at both 404 nm (Soret band) and 668 nm (Q-band) was observed, thus allowing to consider these new chlorin derivatives as photo-stable under visible light irradiation (Figure 2).

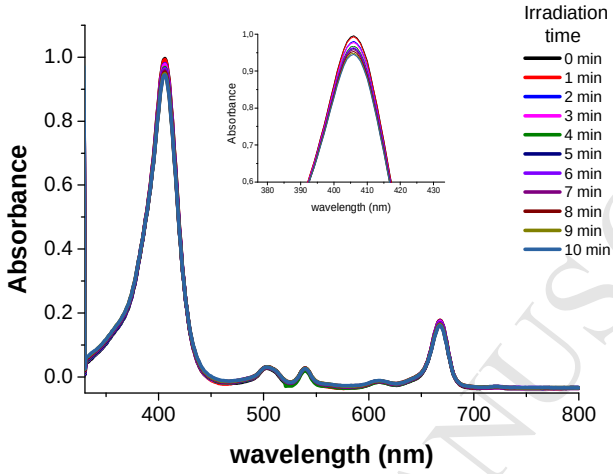

Fig. 2. Photobleaching study of the chlorin **8-a** (inset: expansion of Soret band).

3.5 Partition coefficient in 1-octanol/PBS (Log P)

The lipophilicity of the synthesised chlorin derivatives and verteporfin was determined from the partition coefficient. The log P is defined as the ratio of concentrations of the photosensitiser at equilibrium between the organic and aqueous phases [55, 56]. This feature is important since it allows the incorporation of molecules within the cell. Compounds **8-a**, **8-b** and verteporfin were solubilised in 1-octanol relative to the aqueous phase (PBS). The log P for each compound was calculated according to an adaptation of the method first proposed by Pooler and Valenzeno [57], because the studied photosensitisers are sparingly soluble in the aqueous phase (Equation 3).

$$\log P = \log \frac{(A_{\lambda d})}{(A_{\lambda o} - A_{\lambda d})} \quad (3)$$

Where $A_{\lambda o}$ is the absorption solution before the partition and $A_{\lambda d}$ is the absorption solution after the partition at wavelength 404 nm. Positive log P values mean that the compound exhibit lipophilic characteristics (log P > 0) and negative log P values mean that it shows a hydrophilic character (log P < 0) (Table 2). The photosensitiser candidates **8-a** and **8-b** were less lipophilic than verteporfin when the absorption spectrum before and after partition was considered. This means that a number of molecules of chlorin (**8-a** or **8-b**) were transferred toward the aqueous phase, resulting in stronger amphiphilic characteristics and displaying a stronger interaction with the polar environment [58, 59]. This affinity allows the compounds to diffuse through the aqueous medium and easily across the cell membrane.

Table 2: Partition coefficients using a mixture of 1-octanol and phosphate-buffer saline (PBS). Data are expressed as average ± SD.

Photosensitiser	Partition Coefficient (Log P)
Verteporfin	1.61 ± 0.10
8-a	1.20 ± 0.04*
8-b	1.17 ± 0.03*

* Statistically significant difference from Verteporfin ($p<0.001$)

The chlorins showed amphiphilic characteristics and log-P values that were approximately 25% lower than verteporfin (which presented lipophilic characteristics). This result shows the importance of hydrophilic groups attached to the chlorin structure, which increases the solubility in an aqueous medium without changing the penetration power through the plasmatic

membrane of cells. Once verteporfin has no hydrophilic groups in its structure, it becomes more lipophilic and less soluble in aqueous medium. This result is also consistent with the determined Φ_Δ values.

3.6 Aggregation study

The concentrations of **8-a**, **8-b** and verteporfin analysed by UV-Vis spectroscopy were on the same scale of those used in the cytotoxic assays. Chlorin derivatives **8-a** and **8-b** exhibited no aggregation in an aqueous medium (PBS) of up to 10 μmol L^{-1}because the “L shape” of the molecules prevented some π-stacking interactions (Figure 4A and 4B). Verteporfin showed a shift of 20 nm in the Soret band, which was caused when the strong interactions of the π-orbitals of the aromatic ring induced aggregation (Figure 3) [40]. Once again, the synthesised photosensitiser candidates appeared to be more adequate options for PDT.

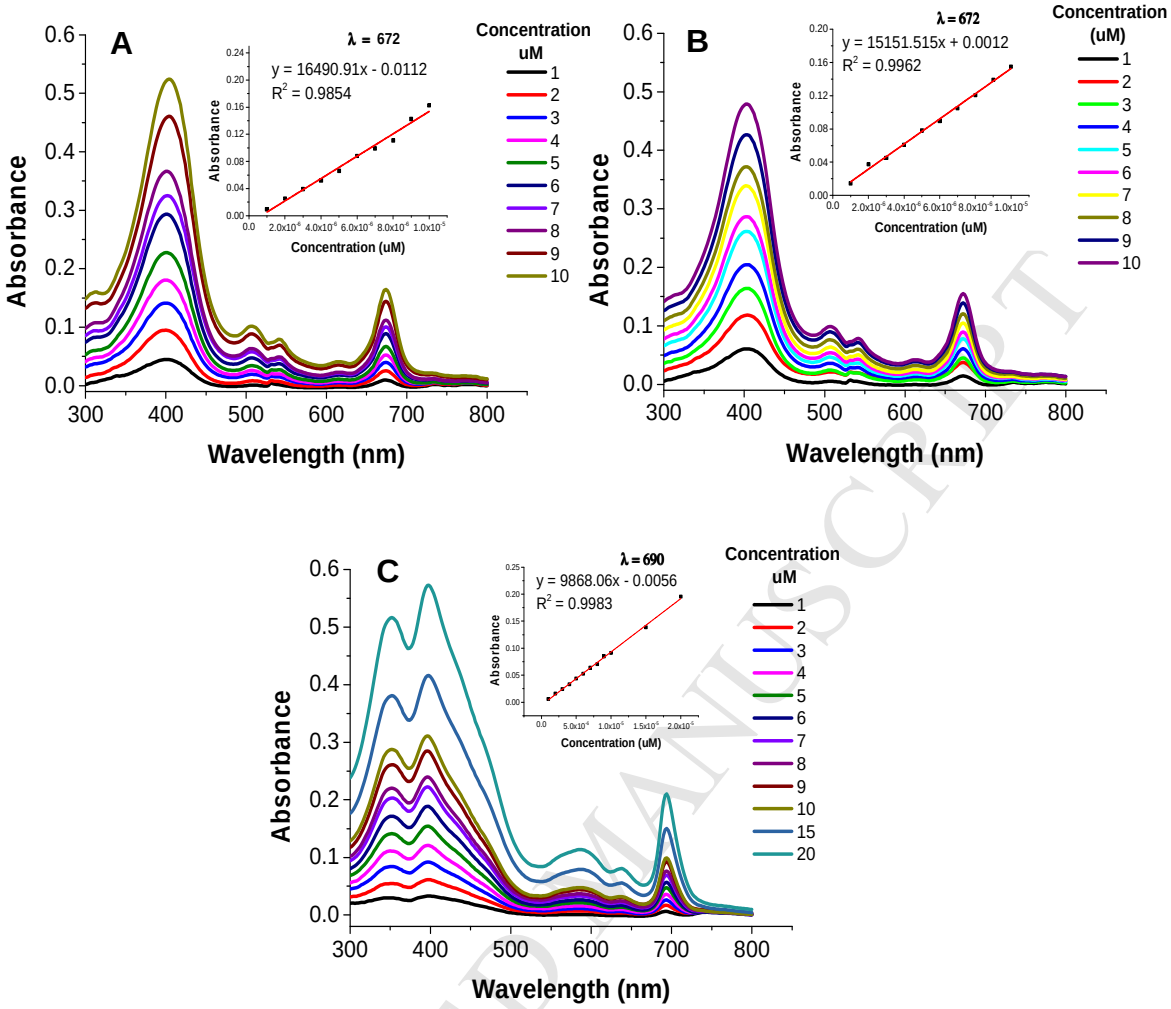

Fig. 3. Aggregation study of (A) Chlorin **8-a** (B) Chlorin **8-b** and (C) Verteporfin in PBS by UV-Vis spectroscopy.

3.7 Phototoxicity assay

The phototoxic assays of **8a**, **8-b** and verteporfin were performed at two light doses (3 and 6 J cm^{-2}) with a light intensity of 27.6 mW cm^{-2} in the tumour cell lines HEp-2 and HeLa and in the non-tumour cells Vero. These assays were important for the determination of the medium inhibitory concentrations (IC_{50}) of each molecule using the MTT colorimetric method.

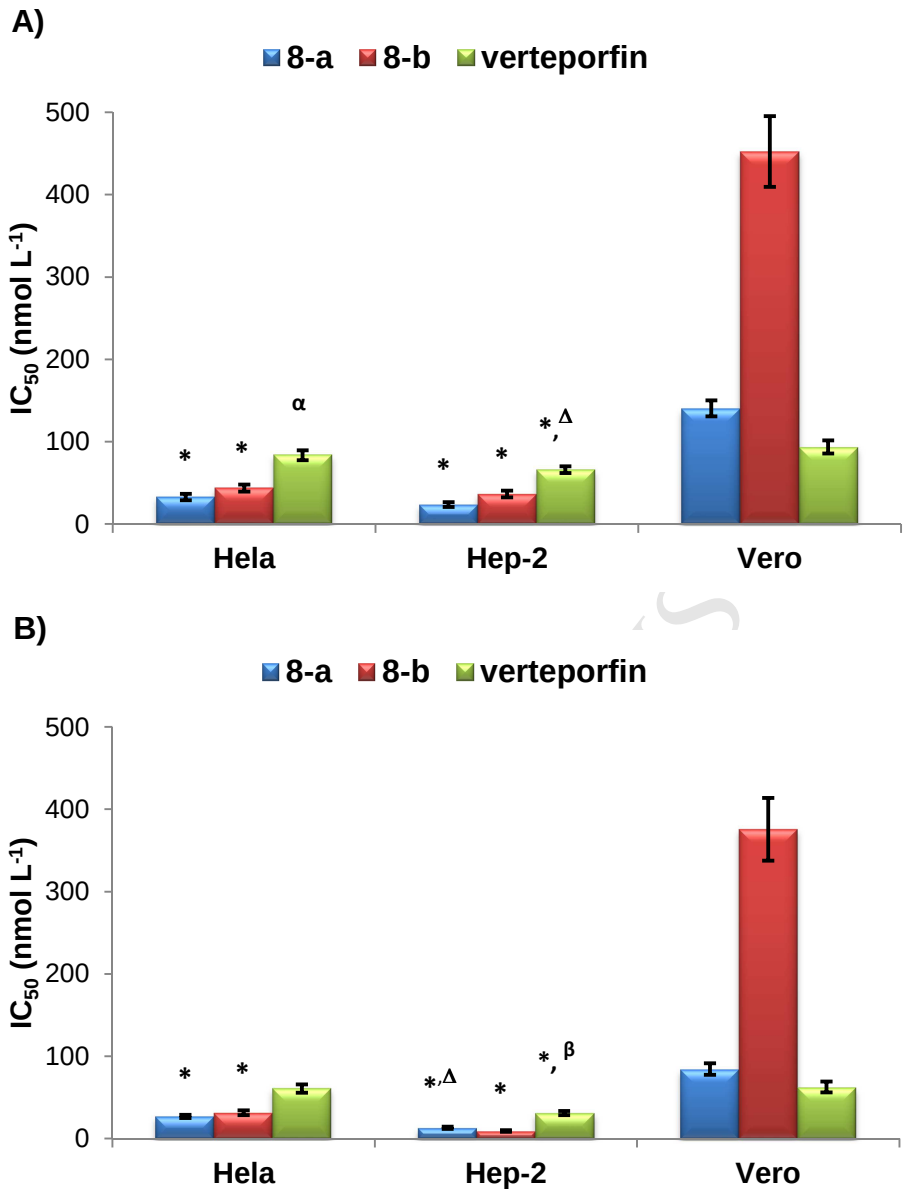

Fig. 4. Medium inhibitory concentrations (IC_{50}) of the chlorins **8-a**, **8-b** and verteporfin in HeLa, HEp-2 and Vero cells. The cells were incubated for 2 h, following by red irradiation (660 nm) and light doses at (A) 3 and (B) 6 J cm^{-2}. The MTT assay was performed to determine the cell viability after 48 h of irradiation. The results are expressed as means ± standard deviation (SD). ***, α**: statistically significant difference from Vero cells ($p<0.001$; $p<0.05$). **Δ, β**: statistically significant difference from HeLa cells ($p<0.01$; $p<0.001$).

Compounds **8-a**, **8-b** and verteporfin showed a lower cytotoxicity in normal cell lines (Vero) for the two tested light doses (Fig. 4), indicating a good selectivity for the tumour cell. This can be due to various factors such as an increase in the permeability of tumour cells, which has been observed in many experiments using animal models [60]. In addition, the location of photosensitisers within the tumour cell may be different compared to normal cells because of the selective retention of each cell such as those with low pH [61], over-expression of low-density lipoprotein receptors [62] (LDL, apoB/E), and the over-expression of some tumour associated macrophages [63]. The chlorin **8-a** showed the lowest IC_{50} value, which means the highest cytotoxicity in HeLa tumour cells (26.9 ± 1.9) at a dose 6 J cm^{-2}, and they were 57% more cytotoxic than verteporfin; the chlorin **8-b** exhibited the lowest value of IC_{50} in the HEp-2 cells (9.2 ± 1.1), and they were 77% more cytotoxic than verteporfin at the same light dose. Furthermore, the tests were carried out in the dark for the three compounds (8-a, 8-b and verteporfin) which demonstrated a very low cytotoxicity in the studied cells. These achievements highlight the important phototoxic effects of newly synthesised photosensitiser candidates and the promising possibility of using these chlorins in PDT.

3.8 Cell death detection by acridine orange/ethidium bromide (AO/EB) staining

In order to determine the mechanism of cell death, cells were labelled with a mixture of acridine orange and ethidium bromide after 48h irradiation. Cell differentiation was analysed with a 20X objective and treated with $1x10^{-8}$ mol L^{-1} of chlorin **8-a** or **8-b**. The three cell lines (HeLa, HEp-2 and Vero) that were

treated with the shorter irradiation time (3 J cm^{-2}) showed a low percentage of cell death (30%). However, those with the largest irradiation time (6 J cm^{-2}) showed a late apoptotic process (condensation and fragmentation of chromatin stained in orange) and a few cells in a necrotic state (red nuclei stained) caused by the loss of the integrity of the cytoplasm membrane (Figure 5B [a-c]).

Explanations for this difference include the time length of light incidence in order to obtain different light doses using the same light source on molecules photosensitiser (in ground state), leading to different number of molecules in the excited triplet state (PS*) and to generation of reactive oxygen species and the higher oxidative stress in tumour cells [64]. These species play an important role in the intrinsic pathway of apoptosis signalling because mitochondrial DNA damage is responsible for respiratory chain electron [65]. Morphological information observed by differential staining with AO/EB suggests that **8-a** and **8-b** induce cell death by apoptosis in all the studied cell lines. However, the route of induction of apoptosis is not completely understood.

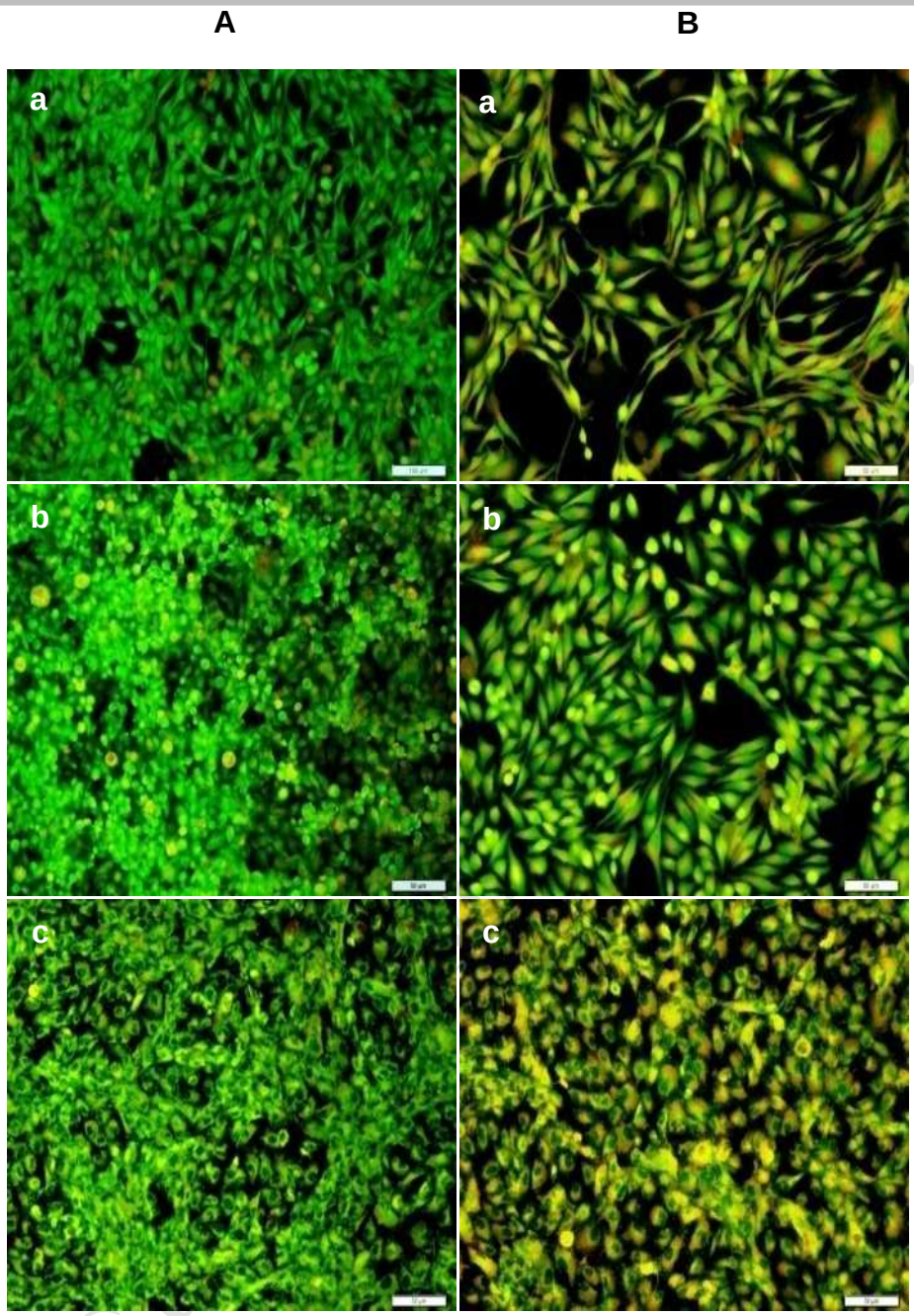

Fig. 5. Fluorescence microscopy images of three cell lines incubated with $1x10^{-8}$ mol L^{-1} chlorin 8-b followed by red light irradiation (660 nm). (**A**) Untreated (control) cells: (a) HeLa (b) HEp-2 and (c) Vero. (**B**) Apoptotic cells after 48h of treatment (6 J cm^{-2}): (a) HeLa (b) HEp-2 and (c) Vero, respectively.

4. Conclusion

In this study, we synthesised two chlorin derivatives, **8-a** and **8-b**, which have an L-shaped structure and are self-prevented from aggregation in aqueous mediums. The photophysical and photochemical properties - for example, singlet oxygen quantum yields, low photobleaching and partition coefficient (log P) made **8-a** and **8-b** better photosensitiser candidates for PDT compared to verteporfin. The cytotoxicity of the chlorin derivatives in the tumour cells was 60% higher than verteporfin, which allowed lower concentrations to be used to have a targeted effect. Fluorescence microscopy showed that the mechanism of cell death occurs by a highly apoptotic process in the three cell lines after irradiation. Therefore, we suggest that the new chlorin derivatives **8-a** and **8-b** exhibit strong potential as photosensitizer, and they should be evaluated further in animal models and other PDT studies.

Acknowledgements

The authors wish to thank the CNPq, FAPESP (2015/21110-4), CEPOF (2013/07276-1) and CAPES for financial support and fellowships, as well as Prof. Ilce Mara de Syllos Cólus for kindly proving the HeLa cell line. We are very grateful to Dr. Mauricio S. Baptista for allow us to do the measurements of singlet oxygen quantum yield in his lab and to Dr. Helena Junqueira for performing the experiments.

References

[1] Asano R, Nagami A, Fukumoto Y, Miura K, Yazama F, Ito H, et al. Synthesis and biological evaluation of new boron-containing chlorin derivatives as agents for both photodynamic therapy and boron neutron capture therapy of cancer. Bioorg Med Chem Lett. 2014;24:1339–43.

[2] Castano AP, Demidova TN, Hamblin MR. Mechanisms in photodynamic therapy: part two-cellular signaling, cell metabolism and modes of cell death. Photodiagnosis Photodyn Ther. 2005;2(1):1–23.

[3] Robertson CA, Evans DH, Abraharnse H. Photodynamic therapy (PDT): a short review on cellular mechanisms and cancer research applications for PDT. J Photochem Photobiol B. 2009;96(1):1–8.

[4] Asano R, Nagami A, Fukumoto Y, Yazama F, Ito H, Sakata I, et al. Synthesis and biological evaluation of new chlorin derivatives as potential photosensitizers for photodynamic therapy. Bioorg Med Chem. 2013;21:2298–304.

[5] Gorman A, Killoran J, O'Shea C, Kenna T, Gallagher WM, O'Shea DF. In vitro demonstration of the heavy-atom effect for photodynamic therapy. J Am Chem Soc. 2004;126:10619–31.

[6] Goncalves NPF, Simoes AVC, Abreu AJ, Abrunhosa AJ, Dabrowski JM, Pereira MM. Synthesis and biological distribution study of a new carbon-11 labeled porphyrin for PET imaging. Photochemical and biological characterization of the non-labeled porphyrin. J Porphyrins Phthalocyanines. 2015;19:946–55.

[7] Dabrowski JM, Pereira MM, Arnaut LG, Monteiro CJ, Peixoto AF, Karocki A, et al. Synthesis, photophysical studies and anticancer activity of a new halogenated water-soluble porphyrin. Photochem Photobiol. 2007;83:897–903.

[8] Ethirajan M, Chen Y, Joshi P, Pandey R. The role of porphyrin chemistry in tumor imaging and photodynamic therapy. Chemic Soc Rev. 2011;40(1):340–62.

[9] Park H, Na K. Conjugation of the photosensitizer Chlorin e6 to pluronic F127 for enhanced cellular internalization for photodynamic therapy. Biomaterials. 2013;34:6992–7000.

[10] Kempa M, Kozub P, Kimball J, Rojkiewicz M, Kus P, Gryczynski Z, et al. Physicochemical properties of potential porphyrin photosensitizers for photodynamic therapy. Spectrochimica Acta A Mol Biomol Spectrosc. 2015;146:249–54.

[11] Simoes AVC, Adamowicz A, Dabrowski JM, Calvete MJF, Abreu AR, Stochel G, et al. Amphiphilicmeso(sulfonate ester fluoroaryl)porphyrins: refining the substituents of porphyrin derivatives for phototherapy and diagnostics. Tetrahedron. 2012;68:8767–72.

[12] Quartarolo AD, Perusse D, Dumoulin F, Russo N, Sicilia E. Hydrophilic annulated dinuclear zinc(II) phthalocyanine as Type II photosensitizers for PDT: a combined experimental and (TD)-DFT investigation. J Porphyrins Phthalocyanines. 2013;17:980–8.

[13] Ongarora BG, Hu X, Li H, Fronczek FR, Vicente MGH. Syntheses and properties of trimethylaminophenoxy-substituted Zn(II)-phthalocyanines. Med Chem Comm. 2012;3:179–94.

[14] Anand S, Ortel BJ, Pereira SP, Hasan T, Maytin EV. Biomodulatory approaches to photodynamic therapy for solid tumors. Cancer Lett. 2012;326(1):8–16.

[15] Dabrowski JM, Arnaut LG. Photodynamic therapy (PDT) of cancer: from local to systemic treatment. Photochem Photobiol Sci 2015;14:1765–80.

[16] Li K, Guo C, Chen Q. Efficient One-Pot Regioselective Synthesis of 2,3-Dibromo-5,10,15,20-tetraarylporphyrins from 5,10,15,20-Tetraarylchlorins. Synlett. 2009:2867–71.

[17] de Assis FF, de Souza JM, Assis BHK, Brocksom TTJ, de Oliveira K. Synthesis and photophysical studies of a chlorin sterically designed to prevent self-aggregation. Dyes Pigments. 2013;98:153–9.

[18] Yoon I, Kim JH, Li JZ, Lee WK, Shim YK. Efficient Photosensitization by a chlorin-polyoxometalate supramolecular complex. Inorg Chem. 2014;53(1):3–5.

[19] Isakau HA, Parkhats MV, Knyukshto VN, Dzhagarov BM, Petrov EP, Petrov PT. Toward understanding the high PDT efficacy of chlorin e6-polyvinylpyrrolidone formulations: photophysical and molecular aspects of photosensitizer-polymer interaction *in vitro*. J Photochem. Photobiol B. 2008;92:165–74.

[20] Szurko A, Rams M, Sochanik A, Sieron-Stoltny K, Kozielec AM, Montforts FP, et al. Spectroscopic and biological studies of a novel synthetic chlorin derivative with prospects for use in PDT. Bioorg Med Chem. 2009;17:8197–205.

[21] Lu F, Hu Z, Sinard J, Garen A, Adelman RA. Factor VII-verteporfin for targeted photodynamic therapy in a rat model of choroidal neovascularization. Invest Ophthalmol Vis Sci. 2009;50:3890–6.

[22] Maruko I, Iida T, Sugano Y, Saito M, Sekiryu T. Subfoveal retinal and choroidal thickness after verteporfin photodynamic therapy for polypoidal choroidal vasculopathy. Am J Ophthalmol. 2011;151:594–603.

[23] Ericson M, Grapengiesser S, Gudmundson F, Wennberg A, Larko O, Moan J, et al. A spectroscopic study of the photobleaching of protoporphyrin IX in solution. Laser Med Sci. 2003;18(1):56-62.

[24] Eshghi H, Sazgarnia A, Rahimizadeh M, Attaran N, Bakavoli M, Soudmand S. Protoporphyrin IX-gold nanoparticle conjugates as an efficient photosensitizer in cervical cancer therapy. Photodiagnosis Photodyn Ther. 2013;10:304–12.

[25] Pavlov VY. Modern aspects of the chemistry of protoporphyrin IX. Russian J Org Chem. 2007;43(1):1–34.

[26] Karim SP, Adelman RA. Profile of verteporfin and its potential for the treatment of central serous chorioretinopathy. Clin Ophthalmol. 2013;7:1867–75.

[27] Mak ST, Wong AC. Single-session combined photodynamic therapy with verteporfin and intravitreal anti-vascular endothelial growth factor therapy for chronic central serous chorioretinopathy: a pilot study at 12-month follow-up. Graefes Arch Clin Exp Ophthalmol. 2013;251:401–2.

[28] Nowak-Sliwinska P, Karocki A, Elas M, Pawlak A, Stochel G, Urbanska K. Verteporfin, photofrin II, and merocyanine 540 as PDT photosensitizers

against melanoma cells. Biochem Biophys Res Commun. 2006;349:549–55.

[29] Juarranz A, Jaen P, Sanz-Rodriguez F, Cuevas J, Gonzalez S. Photodynamictherapy of cancer. Basic principles and applications. Clin Transl Oncol. 2008;10:148–54.

[30] Silbergleit AK, Somers ML, Schweitzer VG, Gardner GM, Peterson E. Vocal fold vibration after photofrin-mediated photodynamic therapy for treatment of early-stage laryngeal malignancies. J Voice. 2013;27:762–4.

[31] Paszko E, Vas GM, Ehrhardt C, Senge MO. Transferrin conjugation does not increase the efficiency of liposomal Foscan during in vitro photodynamic therapy of oesophageal cancer. Eur J Pharm Sci. 2013;48:202–10.

[32] Leung WN, Sun X, Mak NK, Yow CM. Photodynamic effects of mTHPC on human colon adenocarcinoma cells: photocytotoxicity, subcellular localization and apoptosis. Photochem Photobiol. 2002;75:406–11.

[33] Usuda J, Kato H, Okunaka T, Furukawa K, Honda H, Suga Y, et al. Photodynamic therapy using Laserphyrin for centrally located early stage lung cancer. J Clin Oncol. 2006;24(18):7229.

[34] Namatame H, Akimoto J, Matsumura H, Haraoka J, Aizawa K. Photodynamic therapy of C6-implanted glioma cells in the rat brain employing second-generation photosensitizer talaporfin sodium. Photodiagnosis Photodyn Ther. 2008;5:198–209.

[35] Josefsen LB, Boyle RW. Photodynamic therapy and the development metal-based photosensitisers. Met Based Drugs. 2008;2008:1–23.

[36] Allison PR, Sibata CH. Oncologic photodynamic therapy photosensitizers: a clinical review. Photodiagnosis Photodyn Ther. 2010;7:61–75.

[37] Yano S, Hirohara S, Obata M, Hagiya Y, Ogura S, Ikeda A, et al. Current states and future views in photodynamic therapy. J Photochem Photobiol C-Photochem Rev. 2011;12(1):4–67.

[38] dos Santos FAB, Uchoa AF, Baptista MS, Iamamoto Y, Serra OA, Brocksom TJ, et al. Synthesis of functionalized chlorins sterically-prevented from self-aggregation. Dyes Pigments. 2013;99:402–11.

[39] de Oliveira KT, Silva AMS, Tome AC, Neves MGPMS, Neri CR, Garcia VS, et al. Synthesis of new amphiphilic chlorin derivatives from protoporphyrin-IX dimethyl ester. Tetrahedron. 2008;64:8709–15.

[40] Nakae Y, Fukusaki E, Kajiyama S, Kobayashi A, Nakajima S, Sakata I. Syntheses and screening tests of new chlorin derivatives as photosensitizer. J Photochem Photobiol A-Chem. 2005;174:187–93.

[41] Uchoa AF, de Oliveira KT, Baptista MS, Bortoluzzi AJ, Iamamoto Y, Serra OA. Chlorin photosensitizers stericallydesigned to prevent self-aggregation. J Organ Chem. 2011;76:8824–32.

[42] Armarego WLF, Chai CLL. Purification of laboratory chemicals. 6th ed. Burlington, Massachusetts, USA: Elsevier; 2009.

[43] Engel T, Kickelbick G. Thermoreversible Reactions on Inorganic Nanoparticle Surfaces: Diels-Alder Reactions on Sterically Crowded Surfaces. Chem Materials. 2013;25(2):149–57.

[44] Heath WH, Palmieri F, Adams JR, Long BK, Chute J, Holcombe TW, et al. Degradable cross-linkers and strippable imaging materials for step-and-flash imprint lithography. Macromol. 2008;41:719–26.

[45] Wilkinson F, Helman WP, Ross AB. Rate constants for the decay and reactions of the lowest electronically excited singlet-state of molecular-oxygen in solution. An expanded and revised compilation. J PhysChem Ref Data. 1995;24:663–1021.

[46] Redmond RW, Gamlin JN. A compilation of singlet oxygen yields from biologically relevant molecules. Photochem Photobiol. 1999;70:391–475.

[47] Fery-Forgues S, Lavabre D. Are fluorescence quantum yields so tricky to measure? A demonstration using familiar stationery product. J Chem Ed. 1999;76:1260–4.

[48] Engelmann FM, Rocha SV, Toma HE, Araki K, Baptista MS. Determination of n-octanol/water partition and membrane binding of cationic porphyrins. Int J Pharm. 2007;329(1-2):12–8.

[49] Merlin JL, Azzi S, Lignon D, Ramacci C, Zeghari N, Guillemin F. MTT assays allow quick and reliable measurement of the response of human tumour-cells to photodynamic therapy. Eur J Cancer. 1992;28A:1452–8.

[50] Berridge MV, Tan AS, McCoy KD, Wang R. The biochemical and cellular basis of cell proliferation assays that use tetrazoliumsalts. Biochemica. 1996;4:14–9.

[51] Smith S, Ribble D, Goldstein N, Norris D, Shellman Y, Conn P. A Simple Technique for Quantifying Apoptosis in 96-Well Plates. Lab Methods Cell Biol: Biochem Cell Culture. 2012;112:361–8.

[52] Pellosi D, Tessaro AL, Moret F, Gaio E, Reddi E, Caetano W, et al. Pluronic® mixed micelles as efficient nanocarriers for benzoporphyrin derivatives applied to photodynamic therapy in cancer cells. J Photochem Photobiol A:Chem. 2016;314:143–54.

[53] Nas A, Fandakli S, Kantekin H, Demirbas A, Durmus M. Novel organosoluble metal-free and metallophthalocyanines bearing triazole moieties: Microwave assisted synthesis and determination of photophysical and photochemical properties. Dyes Pigments. 2012;95(1):8–17.

[54] Correa JC, Bagnato VS, Imasato H, Perussi JR. Previous illumination of a water soluble chlorine photosensitizer increases its cytotoxicity. Laser Phys. 2012;22:1387–94.

[55] Ferreira J, Menezes PFC, Kurachi C, Sibata C, Allison RR, Bagnato VS. Photostability of different chlorine photosensitizers. Laser Phys Lett. 2008;5:156–61.

[56] Smith DA, Allerton C, Kalgutkar AS, Waterbeemd H, Walker DK, Mannhold R, et al., editors. Pharmacokinetics and metabolism in drug design. 3rd ed. Weinheim, Germany: WILEY-VCH; 2012.

[57] Pooler J, Valenzeno D. Physicochemical determinants of the sensitizing effectiveness for photooxidation of nerve membranes by fluorescein derivatives. Photochem Photobiol. 1979;30:491–8.

[58] Shah SS, Laghari GM, Naeem K, Shah SWH. Partition coefficient of amphiphilic chemicyanine dyes between the aqueous and the micellar phase of sodium dodecyl sulfate by differential absorbance spectroscopy. Colloids Surfaces A: Physicochem Eng Aspects. 1998;143(1):111–5.

[59] Kepczynski M, Pandian RP, Smith KM, Ehrenberg B. Do liposome-binding constants of porphyrins correlate with their measured and predicted partitioning between octanol and water? Photochem Photobiol. 2002;76(2):127–34.

[60] Yuan F, Leunig M, Berk DA, Jain RK. Microvascular permeability of albumin, vascular surfacearea, and vascular volume measured in human adenocarcinoma LS174T using dorsal chamber in SCID mice. Microvasc Res. 1993;45:269–89.

[61] Castano AP, Demidova TN, Hamblin MR. Mechanisms in photodynamic therapy: Part three- Photosensitizer pharmacokinetics, biodistribution, tumor localization and modes of tumor destruction. Photodiagnosis Photodyn Ther. 2005;2(2):91–106.

[62] Allison B,A Pritchard PH, Levy JG. Evidence for low-density lipoprotein receptor-mediated uptake of benzoporphyrin derivative. Br J Cancer. 1994;69:833–9.

[63] Korbelik M, Krosl G. Photofrin accumulation in malignant and hostcell populations of a murine fibrosarcoma. Photochem Photobiol. 1995;62(1):162–8.

[64] Dai T, Fuchs BB, Coleman JJ, Prates RA, Astrakas C, St Denis TG, et al. Concepts and principles of photodynamic therapy as an alternative antifungal discovery platform. Front Microbiol. 2012;3:1–16.

[65] Fruehauf JP, Meyskens FL Jr. Reactive oxygen species: a breath of life or death? Clin Cancer Res. 2007;13:789–94.